[4] W. L. Jung and Jingshown Wu, "Stable broadband microwave amplifier design," *IEEE Trans. Microwave Theory Tech*, vol. 38, pp. 1079–1085, Aug. 1990.
[5] H. J. Carlin, "A new approach to gain-bandwidth problems," *IEEE Trans. Circuits Syst.*, vol. CAS-24, pp. 170–175, Apr. 1977.
[6] B. S. Yarman, "A dynamic CAD technique for designing broadband microwave amplifiers," *RCA Review*, vol. 44, pp. 551–565, Dec. 1983.
[7] IMSL User's Manual, MATH/LIBRARY&\trade; , FORTRAN subroutines for mathematical applications, version 1.1, Jan. 1989. IMSL customer relations, Houston.
[8] K. M. Brown and J. E. Dennis, "Derivative free analogues of the Levenberg–Marquardt and Guass algorithms for nonlinear least square approximations," *Numerische Mathematik*, vol. 18, p. 289, 1972.
[9] H. J. Carlin, and J. J. Komiak, "A new method of Broad-band equalization applied to microwave amplifiers," *IEEE Trans. Microwave Theory Tech.*, vol. MTT-27, pp. 93–99, Feb. 1979.
[10] M. S. Ghausi, *Principles and Design of Linear Active Circuits*. New York: McGraw-Hill, 1965.
[11] NEC Corporation, "NE700, low cost Ku-Band GaAs MESFET," 1983, Santa Clara, CA.
[12] W. L. Jung and Jingshown Wu, "Broadband amplifier design with stability consideration," *Int. J Electronics*, vol. 68, no. 2, pp. 209–221, 1990.
[13] EESOF, Touchstone^{R}, User's Manual, EESOF Inc., West Lake Village, CA 91362, Aug. 1986.
[14] G. C. Temes and J. W. LaPatra, *Introduction to Circuit Synthesis and Design* New York: McGraw-Hill, 1977.
[15] T. R. Cuthbert JR, *Optimization Using Personal Computers with Applications to Electrical Networks*. New York: Wiley, 1987.

Extraction of Device Noise Sources from Measured Data Using Circuit Simulator Software

Pertti K. Ikalainen

***Abstract*— A procedure is presented for extracting the properties of device noise sources from experimental data. The extraction procedure can be implemented using commercially available circuit simulators. An example concerning a low-noise pseudomorphic HEMT shows that the two noise sources extracted from experimental data are largely uncorrelated provided that parasitic elements are de-embedded from the measurement and that the sources are extracted in H-parameter format.**

I. Introduction

It is usual to characterize the noise performance of a microwave device with four noise parameters: minimum noise figure $F_{\min}$, optimum source admittance Y_{opt}, and equivalent noise resistance R_n. Together with S-parameters they completely characterize the small-signal performance of any two-port device. However, it is sometimes desirable and physically more meaningful to examine the noise performance in terms of two noise sources associated with the two-port. The four parameters then become the strength of the two sources and the (complex) cross-correlation between them. These two sources can be separated from the two-port in a number of ways, and the theoretical procedures for treating these cases are well established [1], [2].

Given experimental noise parameters (in terms of $F_{\min}, Y_{opt}$, and R_n) and S-parameters, we need an extraction procedure to find the properties of the noise sources. It is also frequently desirable to de-embed the effects of known device parasitics before extracting the noise sources. One such de-embedding and extraction procedure was presented for FETs in [3]. However, that method requires software for conversion between Z and Y correlation matrices. It is the purpose of this paper to report a simple extraction method using commercially available circuit simulation software. This method is general and works for any kind of two port device.

Manuscript received March 30, 1992; revised June 19, 1992.

The author is with Texas Instruments Incorporated, P.O. Box 655936, MS 134, Dallas, TX 75265.

IEEE Log Number 9204469.

II. Extraction of Noise Sources From Measured Data

Consider the noise equivalent representation of Fig. 1(a) [1], [2]. Since knowledge of the strength and cross-correlation of the two noise current sources along with the Y-parameters of the network uniquely determines the four noise parameters, it then follows that, conversely, the noise currents can be uniquely determined from a knowledge of the Y-parameters and the four noise parameters. Equations could be written for the noise sources directly in terms of Y-parameters and $F_{\min}, Y_{opt}$, and R_n. However, it is convenient to first convert the standard noise parameters $F_{\min}, Y_{opt}$, and R_n into a format compatible with the noise equivalent representation of Fig. 1(b) [1], [2]

$$Y_c = \frac{F_{\min} - 1}{2R_n} - Y_{opt} \tag{1}$$

$$G_n = (F_{\min} - 1)\left(G_{opt} - \frac{F_{\min} - 1}{4R_n}\right), \tag{2}$$

where Y_c is the correlation admittance between i_n and e_n of Fig. 1(b)

$$Y_c = \frac{\langle i_n e_n^* \rangle}{\langle e_n e_n^* \rangle}, \tag{3}$$

and G_n is related to the strength of the completely uncorrelated part i_{nu} of i_n of Fig. 1(b)

$$G_n = \frac{\langle |i_{nu}|^2 \rangle}{4kT_0B} = \frac{\langle |i_n - Y_c e_n|^2 \rangle}{4kT_0B}, \tag{4}$$

where k is the Boltzmann constant, T_0 is the standard reference temperature of 290 K, and B is the incremental bandwidth. The brackets $\langle\,\rangle$ indicate time average and * indicates complex conjugation. R_n is related to the strength of e_n of Fig. 1(b) by

$$R_n = \frac{\langle |e_n|^2 \rangle}{4kT_0B}, \tag{5}$$

We now can write equations for i_{n1} and i_{n2} of Fig. 1(a) in terms of R_n, G_n, and Y_c utilizing definitions (3)–(5) and the transformation [2] between i_{n1} and i_{n2} of Fig. 1(a), and i_n and e_n of Fig. 1(b), respectively,

$$\langle |i_{n1}|^2 \rangle = 4kT_0B(G_n + R_n|Y_{11} - Y_c|^2) \tag{6}$$

$$\langle |i_{n2}|^2 \rangle = 4kT_0BR_n|Y_{21}|^2 \tag{7}$$

$$\frac{\langle i_{n1} i_{n2}^* \rangle}{\sqrt{\langle |i_{n1}|^2 \rangle \langle |i_{n2}|^2 \rangle}} = \frac{Y_{21}^*(Y_{11} - Y_c)}{|Y_{21}|\sqrt{\dfrac{G_n}{R_n} + |Y_{11} - Y_c|^2}}. \tag{8}$$

It is interesting to note that the only Y-parameters that enter into (6)–(8) are Y_{11} and Y_{21}. Equations (1), (2), and (6)–(8) can be programmed in a commercial circuit simulator with "output equation" capability. For example, we have used LIBRA and TOUCHSTONE [4] in the examples discussed later in this paper.

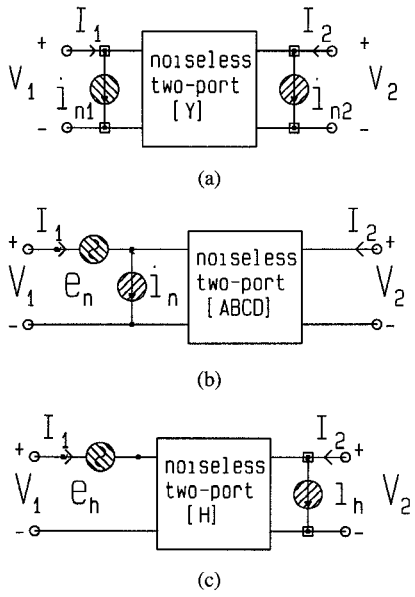

Fig. 1. Noise equivalent representations of a two-port: (a) Two noise current sources in Y-parameter format, (b) one noise current and one noise voltage source in ABDC- or chain matrix format, and (c) one noise current and one noise voltage source in H-parameter format.

Another possible form of presentation, particularly suitable for FETs as we will discuss, is the H-parameter format, see Fig. 1(c),

$$\begin{cases} V_1 = H_{11}I_1 + H_{12}V_2 + e_h \\ I_2 = H_{21}I_1 + H_{22}V_2 + i_h, \end{cases} \tag{9}$$

where

$$\begin{cases} e_h = -\dfrac{1}{Y_{11}} i_{n1} \\ i_h = i_{n2} - \dfrac{Y_{21}}{Y_{11}} i_{n1}. \end{cases} \tag{10}$$

e_h and i_h are new noise sources corresponding to input open-circuited noise voltage (with output shorted) and output short-circuited noise current (with input open). Noise source extraction formulas can be derived from (10) and (6)–(8) to arrive at

$$\langle |e_h|^2 \rangle = \frac{4kT_0B(G_n + R_n|Y_{11} - Y_c|^2)}{|Y_{11}|^2} \tag{11}$$

$$\langle |i_h|^2 \rangle = 4kT_0B \left| \frac{Y_{21}}{Y_{11}} \right|^2 (G_n + R_n|Y_c|^2) \tag{12}$$

$$\frac{\langle e_h i_h^* \rangle}{\sqrt{\langle |e_h|^2 \rangle \langle |i_h|^2 \rangle}} = \frac{Y_{21}^*}{|Y_{21}|} \frac{G_n + R_n Y_c^* (Y_c - Y_{11})}{\sqrt{(G_n + R_n|Y_{11} - Y_c|^2)(G_n + R_n|Y_c|^2)}} \tag{13}$$

III. De-Embedding of Parasitics

If device parasitics are known (e.g., through independent measurements or modeling), they can be de-embedded before the extraction. All that needs to be done is to add elements with negative values and in reverse order to the measured two-port data. This process is illustrated in Fig. 2 for the example to be discussed next. Note that the temperature of the resistive elements has to be equal to the actual ambient temperature of the measurement. A word of caution is necessary with regard to use of commercial software here. It is unusual to have negative resistances in a noise equivalent circuit, and it is conceivable that the software may not de-embed their noise contribution properly. However, we have determined that at least LIBRA and TOUCHSTONE do correctly de-embed resistive elements using this approach.

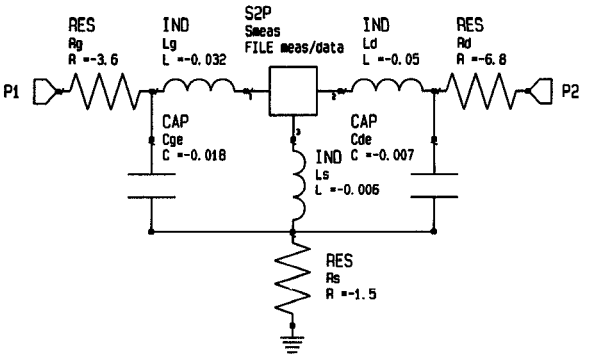

Fig. 2. Parasitic elements can be de-embedded from measured data by connecting negative elements in reverse order.

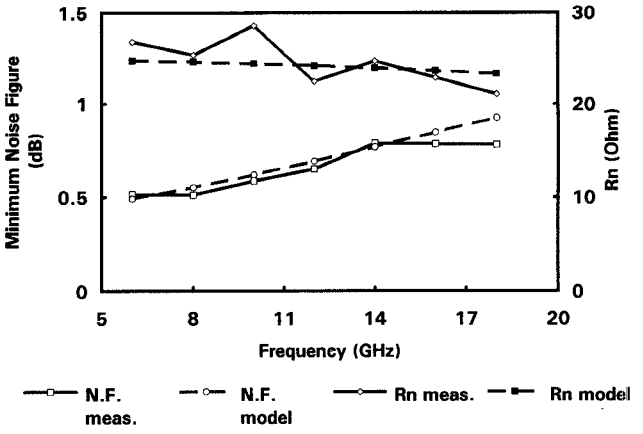

Fig. 3. Measured and modeled $F_{\min}$ and R_n of the PHEMT shown in Fig. 5.

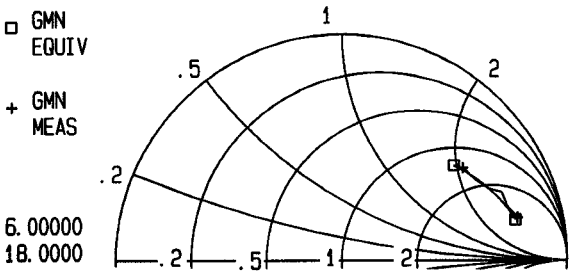

Fig. 4. Measured and modeled optimum source reflection coefficient Γ_{opt} of the PHEMT shown in Fig. 5.

IV. Example

S-parameters and noise parameters were measured on-wafer from a 0.25-μm gate length (75-μm width) GaAs-based pseudomorphic HEMT (PHEMT). Measured noise parameters are shown in Figs. 3 and 4. (The modeled data in Figs. 3 and 4 is to be discussed later.) As is obvious from Figs. 3 and 4, there is quite a lot of scatter in the on-wafer noise parameter measurement which, at least according to our experience, is not unusual in automated on-wafer noise parameter measurements on a small device with very low noise figure. That same scatter shows up, of course, in the extracted noise sources. However, general trends in the data can still be usefully examined.

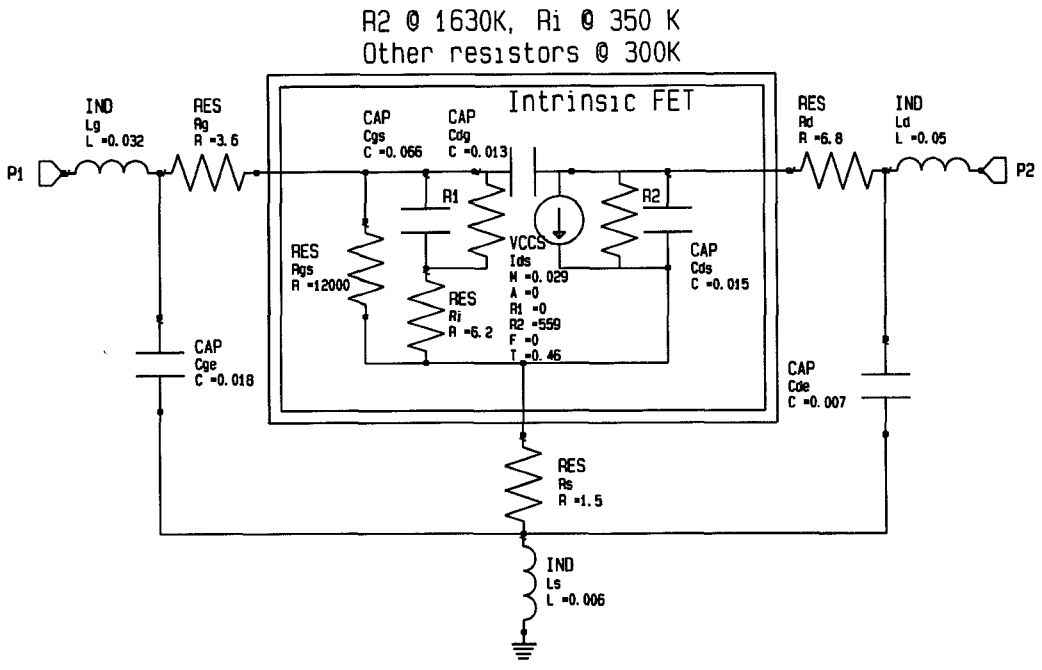

Fig. 5. Equivalent circuit of our pseudomorphic HEMT. R1 is the "sense" element of the voltage-controlled current source VCCS. Making R1 = 0 makes the simulator treat R1 as infinite. Capacitors are in pF and inductors are in nH.

A circuit model, shown in Fig. 5, was developed from S-parameters and additional "cold-FET" measurements to determine parasitic elements [5]. The noise extraction procedure was then applied to the measured data. First all parasitic elements were de-embedded from the data as shown in Fig. 2. Elements Rgs and Cdg of Fig. 5 were de-embedded, as well, by continuing the process indicated in Fig. 2. Cdg was de-embedded to remove its effects on the correlation between the noise sources. De-embedding Rgs gave flatter noise source spectra at low frequencies. It is believed that Rgs represent the small forward conductance of the gate Schottky (the device was enhancement mode and had to be biased with positive voltage at the gate). After de-embedding, the noise sources were extracted in both Y- and H-parameter format. The results are shown in Figs. 6–9. Fig. 6 shows the magnitudes of i_{n1} and i_{n2}. i_{n2} is observed to be fairly constant over the frequency range while i_{n1} shows a characteristic frequency dependence, both in accordance with theory [6]. Fig. 7 shows the correlation coefficient between i_{n1} and i_{n2}. The real part of the correlation is seen to be small compared to the imaginary part, and the imaginary part has only slight frequency dependence, again in accordance with theory [6].

According to the theory of [7] the frequency dependence of i_{n1} and the correlation between i_{n1} and i_{n2} in the Y-parameter format mostly arises from the use of short-circuit condition at the input of an FET as that allows gate noise current flow through C_{gs}. Using H-parameter format, instead, should show constant open-circuit noise voltage at the gate, constant short-circuit noise current at the drain, and little correlation between the two. That is indeed seen to be the case in Figs. 8 and 9. Using an open circuit condition at the gate while extracting the noise sources from experimental data is seen to undo most of the correlation between input and output noise. It should be noted that de-embedding all the parasitics and Cdg is essential to obtaining the correlation properties of the assumed internal sources.

The circuit model shown in Fig. 5 can be used to model the noise performance by assigning temperatures to the resistors [7]. Based on the H-parameter noise sources, the average strength of drain noise current is approximately 160 $(\text{pA})^2/\text{Hz}$ while the gate noise voltage

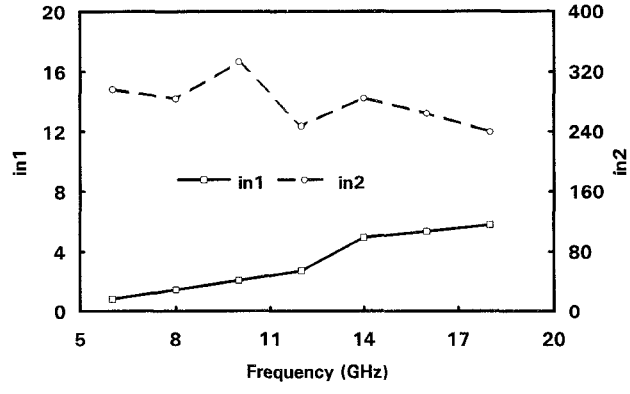

Fig. 6. The strength of two noise current sources in $(\text{pA})^2/\text{Hz}$ as extracted from measured data in Y-parameter format. Parasitic elements and Cdg and Rgs shown in Fig. 5 have been de-embedded.

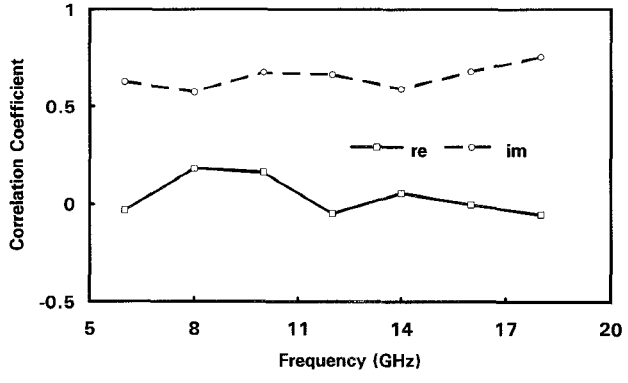

Fig. 7. The correlation coefficient between the two noise current sources shown in Fig. 6 as extracted from measured data.

is approximately 0.12 $(\text{nV})^2/\text{Hz}$, see Fig. 8. These correspond to temperature 1630 K for Rds and 350 K for Ri. All other resistors are at 300 K. Measured and modeled noise parameters are compared

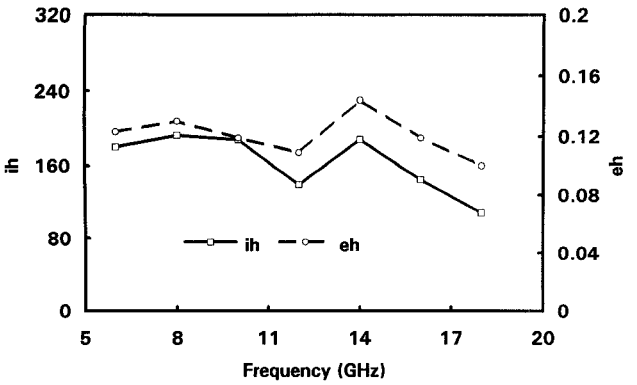

Fig. 8. The strength of a noise current source in $(pA)^2/Hz$ and a noise voltage source in $(nV)^2/Hz$ as extracted from measured data in H-parameter format. Parasitic elements and Cdg and Rgs shown in Fig. 5 have been de-embedded.

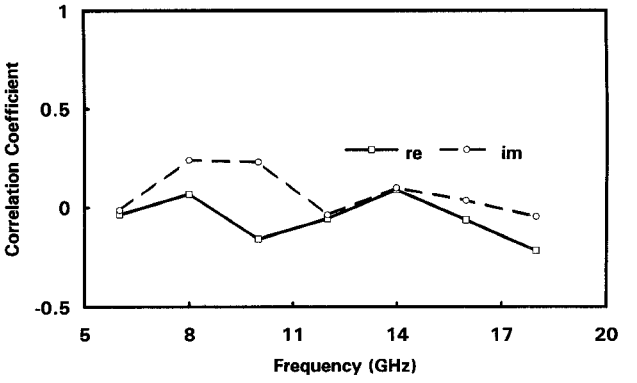

Fig. 9. The correlation coefficient between the noise current source and the noise voltage source shown in Fig. 8 as extracted from measured data.

in Figs. 3 and 4. Quite good agreement is observed. Several other HEMTs have been analyzed and modeled with similar results.

V. Conclusions

A procedure for noise source extraction from measured data was presented. Experimental data from a low-noise HEMT device showed little correlation between input and output noise when the noise sources were extracted in H-parameter format forcing open-circuit conditions at the gate and short-circuit conditions at the drain. The experimental data show that an accurate HEMT noise model may be constructed using non-correlated noise sources.

Acknowledgment

The author wishes to thank Dr. Paul Saunier for device fabrication and Mr. Mark A. Walker for noise parameter measurements.

References

[1] H. A. Haus (Chairman), "Representation of noise in linear two-ports," *Proc IRE*, vol. 48, pp. 69–74, Jan. 1960.
[2] H. Rothe and W. Dahlke, "Theory of noisy fourpoles," *Proc. IRE*, vol. 44, pp. 811–818, June 1956.
[3] A. Riddle, "Extraction of FET model noise-parameters from measurement," in *1991 IEEE MTT-S Int. Microwave Symp. Dig.*, pp. 1113–1116.
[4] Circuit simulator software available from EEsof, Inc., Westlake Village, CA 91362.
[5] G. Dambrini *et al.*, "A new method for determining the FET small-signal equivalent circuit," *IEEE Microwave Theory Tech.*, vol. 36, no. 7, pp. 1151–1159, July 1988.
[6] R. A. Pucel, H. A. Haus, and H. Statz, "Signal and noise properties of gallium arsenide microwave field-effect transistors," in *Advances in Electronics and Electron Physics*, vol. 38, L. Morton, Ed., New York: Academic Press, 1975.
[7] M. W. Pospieszalski, "Modeling of noise parameters of MESFET's and MODFET's and their frequency and temperature dependence," *IEEE Trans Microwave Theory Tech.*, vol. 37, pp. 1340–1350, Sept. 1989.

An Efficient Method for the Determination of Resonant Frequencies of Shielded Circular Disk and Ring Resonators

Faton Tefiku and Eikichi Yamashita

Abstract— **This short paper describes an efficient method for the determination of resonant frequencies of shielded circular disks and annular ring resonators. Bounary integral equations are set up based on the Green's identity in the circular cylindrical coordinates, and are numerically solved by discretizing common boundary integral paths. The overall integration path is considerably shortened to reduce computation time by using simple eigen functions satisfying regular homogeneous boundary conditions as weighting functions instead of using Green's functions. Computational results for both circular disks and annular rings are presented and compared with other available numerical results for some cases. This method can be extended to treat thick conductors.**

I. Introduction

Circular disks and annular ring conductors printed on a dielectric substrate are finding a wide range of applications in microwave integrated circuits. Various simple models have been employed in the past to estimate the resonant frequencies of these structures: a simple cavity model with magnetic side walls [1], [2], a modified cavity model [3], a planar waveguide model [4] [5] taking into account fringe fields for both circular disk and annular ring resonators. A more rigorous method was developed for an annular ring using the reaction concept [6]. With a full wave analysis in the Hankel transform domain it was possible to estimate both resonant frequencies and radiation patterns [7], [8]. Calculations have also been made under the assumption of a conductive shielding in the case of resonator structures with high dielectric permittivities or thin substrates [9], [10].

The boundary integral equation method without using Green's function has been proposed [11] and has recently been employed in the analysis of planar transmission lines [12]. It is one of the features of the method that eigen functions satisfying the regular boundary conditions of the shielding conductor are used instead of Green's function. The manipulation with complicated Green's functions is avoided in this way and the overall integration path is considerably shortened for saving the computational time.

In this short paper, we develop the above boundary integral equation method in the circular cylindrical coordinates to solve

Manuscript received March 16, 1992; revised May 26, 1992.
The authors are with the Department of Electronic Engineering, University of Electro-Communications, Chofugaoka 1-5-1, Chofu-Shi, Tokyo 182, Japan.
IEEE Log Number 9204494.